Viability assessment of large-scale Claude cycle hydrogen liquefaction
A study on technical and economic perspective

Tamarona, Panji B.; Pecnik, Rene; Ramdin, Mahinder

DOI
10.1016/j.ijhydene.2024.06.021

Publication date
2024

Document Version
Final published version

Published in
International Journal of Hydrogen Energy

Citation (APA)
Tamarona, P. B., Pecnik, R., & Ramdin, M. (2024). Viability assessment of large-scale Claude cycle hydrogen liquefaction: A study on technical and economic perspective. *International Journal of Hydrogen Energy*, *77*, 383-396. https://doi.org/10.1016/j.ijhydene.2024.06.021

International Journal of Hydrogen Energy 77 (2024) 383–396

Contents lists available at ScienceDirect

International Journal of Hydrogen Energy

journal homepage: www.elsevier.com/locate/he

Viability assessment of large-scale Claude cycle hydrogen liquefaction: A study on technical and economic perspective

Panji B. Tamarona, Rene Pecnik, Mahinder Ramdin *

Process and Energy Department, Delft University of Technology, Leeghwaterstraat 39, 2628 CB Delft, The Netherlands

ARTICLE INFO

Keywords:
Hydrogen liquefaction
Claude cycle
Process modeling
Preliminary-design
Techno-economic

ABSTRACT

The competitiveness of hydrogen as a sustainable energy carrier depends greatly on its transportation and storage costs. Liquefying hydrogen offers advantages such as enhanced purity, versatility, and higher density, yet current industrial liquefaction processes face efficiency and cost challenges. Although various large-scale and efficient liquefaction concepts exist in the literature, they often overlook the economic and technical viability of such plants. Here, we addresses this issue by establishing a framework for modeling a large-scale hydrogen liquefaction concept and conducting both technical and economic assessments, with a specific focus on 125 tonnes per day (TPD) high-pressure hydrogen Claude-cycle concept. The technical analysis involves preliminary designs of key process components, while the economic assessment utilizes Aspen Process Economic Analyzer. Our findings indicate that at an electricity price of €0.1/kWh, the Claude-cycle liquefier concept yields a specific liquefaction cost (SLC) of €1.55/kg_{LH_2}. A sensitivity analysis was performed, which shows that electricity price has a significant influence on the economics. Further investigation on the compressors design shows that incorporating high-speed centrifugal compressors could reduce the SLC by 5.42% and potentially more. Scaling up to 250 and 500 TPD reveals further cost improvements, while cost projections indicate substantial declines as the technology matures. Ultimately, this paper presents novel cost-scaling and experience curves of hydrogen liquefaction technology, demonstrating the compelling economic viability of integrating large-scale hydrogen liquefaction into sustainable energy infrastructure.

1. Introduction

Hydrogen (H_2), as an energy carrier, has the potential to become a key player in a sustainable energy future [1]. However, there are still many challenges preventing the widespread use of hydrogen. Transport and storage costs are critical to the competitiveness of hydrogen, as they can significantly increase the final price of hydrogen fuels. Due to its low energy density, gaseous hydrogen from production stage would require an additional physical or chemical conversion process before long-term storage and transportation [2]. Liquefaction is a promising option, as storing and transporting hydrogen in liquid form have several advantages, such as enhanced purity, end use versatility, and high volumetric hydrogen density [2]. Nonetheless, current liquid hydrogen (LH_2) production faces limitations that hinder its global use, including economics and scale constraints.

Most commercial hydrogen liquefaction plants operate with capacities of less than 20 tonnes per day (TPD), with the largest having the capacity of 32 TPD [2]. The specific energy consumption (SEC) of these liquefiers ranges from 10 to 20 kWh/kg_{LH_2} [3], exerting a significant influence on the current hydrogen specific liquefaction costs (SLC), which vary between US$2.5 and US$3.0 per kg_{LH_2} [2,4]. In contrast, the theoretical energy to liquefy hydrogen from ambient (300 K, 1.01 bar) conditions is 3.9 kWh/kg_{LH_2}, including the necessary conversion of ortho- to para-hydrogen [5], indicating that there is ample room for improvement. Recent studies indicate a typical decrease in liquefaction costs with increasing plant capacity, and some estimates suggest the cost could drop to less than US$1.0/$kg_{LH_2}$ [2]. Besides cost reduction, the anticipated rise in global hydrogen demand further strengthens the necessity for larger liquefaction plants.

Numerous conceptual designs for large-scale hydrogen liquefaction plants have been developed, aiming to optimize process efficiency and reduce the overall SEC [2]. These concepts suggest that an SEC target between 6 and 8 kWh/kg_{LH_2} for large-scale liquefiers is achievable without the use of groundbreaking technologies such as quantum plumbing, magnetocaloric, or thermoacoustic liquefaction. However, insufficient attention has been given to the overall expenses of the plant, which is essential to estimate the liquefaction costs, as well as to the technical feasibility of scaling up the components for the required unit operations. Consideration of these factors is crucial, as practical

* Corresponding author.
E-mail address: m.ramdin@tudelft.nl (M. Ramdin).

https://doi.org/10.1016/j.ijhydene.2024.06.021
Received 27 March 2024; Received in revised form 31 May 2024; Accepted 3 June 2024

and economically viable designs are essential for realizing large-scale hydrogen liquefaction facilities. As noted by Berstad et al. [6], the development of new processes should not merely focus on a "race to the bottom" in power requirements; instead, emphasis should be on identifying rational and economically viable pathways for improving efficiency.

The majority of reported hydrogen liquefaction costs have been estimated by projecting the overall capital costs of the process plant, utilizing scaling factors derived from limited historical data [7–14]. Given that this approach solely relies on plant capacity as an input parameter to offer a "ballpark" cost estimation, it proves suboptimal for comparing the costs of different plant configurations, particularly when their capacities are comparable. Feasibility studies sponsored by companies and governments often leverage confidential equipment cost correlations and recent quotations from contractors for the most accurate cost evaluations [15,16]. However, this approach is often impractical for academics and researchers in this field.

In response to these challenges, this study introduces a framework for modeling a large-scale hydrogen liquefaction process and assessing the plant's economic feasibility while strictly addressing existing technical limitations. The research commences by modeling a promising high-capacity hydrogen liquefaction concept using a process simulation tool. Subsequently, preliminary design procedures are developed and implemented for the main equipment to assess the plant's technical feasibility. Utilizing Aspen Process Economic Analyzer (APEA), the study estimates the capital and operating costs based on the model and preliminary designs, followed by a comprehensive economic evaluation. Furthermore, sensitivity and scale-up analyses are conducted to assess the impact of electricity price, compressor's maximum tip speed, and plant capacity on overall efficiency and economics. Finally, the study predicts potential cost and experience curves for hydrogen liquefaction technology, drawing on the cost results of this research and projections from relevant literature.

2. Process modeling

Various large-scale hydrogen liquefaction concepts have been reviewed by Aasadnia & Mehrpooya [17]. Many of these modern investigations focus solely on "pure" process simulation, often overlooking the viability of integral components [18]. Consequently, several proposed liquefaction systems, despite being relatively efficient, are often highly complex and may prove technically or economically unfeasible.

Among the concepts reviewed, the high-pressure hydrogen (HP-H_2) Claude cycle, with a mixed-refrigerant (MR) Joule-Thomson (JT) precooling cycle, as proposed by Cardella et al. [19,20] and Berstad et al. [6], stands out as one of the most promising designs for a near-future implementation [2]. According to the optimization study of Cardella et al. [19,20], the SEC of the HP-H_2 Claude liquefier can be reduced to about 6 kWh/kg, concurrently decreasing the SLC by nearly 67% compared to small-scale 5 TPD plants, reaching below €1/kg. Furthermore, the adoption of the MR precooling system eliminates the need for the liquid nitrogen (LN_2) pre-cooling system, which typically accounts for considerable portion of the total liquefaction energy [2,21]. Another challenge with the use of LN_2 is the large temperature difference between the cooling and heating curves of hydrogen and nitrogen, limiting heat recovery and increasing irreversibilities [6,22]. In contrast, MRs provide flexibility by allowing adjustments in their composition to minimize temperature discrepancies in heat transfer, thereby enhancing overall thermodynamic efficiency [2,6,19,22].

Based on these factors, the HP-H_2 Claude cycle with MR precooling concept is selected to be the base process in this study. The process is predominantly modeled in reference to the 125 TPD conceptual plant proposed by Berstad et al. [6].

Table 1
Mixed-refrigerant composition [23].

Component	Mole fraction
Nitrogen	0.101
Methane	0.324
Ethane	0.274
Propane	0.031
n-Butane	0.270

Process description

Fig. 1 illustrates the process flow diagram (PFD) of the hydrogen liquefaction process under consideration. Gaseous hydrogen is fed to the process plant at a rate of 125 TPD at 20 bar and 298.15 K. The hydrogen is first cooled by the MR precooling system as it enters the first multi-stream plate-fin heat exchanger (PFHX). The precooling cycle utilizes a five-component refrigerant mixture to cool the hydrogen feed to 114 K. The MR composition, given in Table 1, follows the formulation used by Skaugen et al. [23].

The MR compression in the precooling module involves two compressors equipped with aftercoolers. The aftercoolers cools incoming streams to 298.15 K with cooling water that is assumed to be readily available within the plant. The first MR compressor (MRC), **MRC-1**, pressurizes the MR to 12 bar, and at its aftercooler outlet, the MR partially condenses. A vapor–liquid separator then separates the multiphase stream. The collected liquid condensate is pressurized to 35 bar using a pump, while the vapor flow is compressed by the second MRC to the same pressure. The aftercooler of **MRC-2** partially re-condenses the vapor refrigerant, which then mixes with the pressurized liquid from the pump before entering the heat exchanger. In the PFHX, the multiphase pressurized refrigerant and the hydrogen feed, are cooled to 114 K. The exiting refrigerant is expanded via JT valve to a pressure of 3.6 bar, which accordingly decreases its temperature to 111.3 K. This cold and low-pressure refrigerant is routed back to the cold side of the PFHX to absorb the heat from the two hot streams of pressurized refrigerant and hydrogen feed. This precooling PFHX configuration ensures a tight thermal match between streams, promoting an exergy-efficient heat transfer [6].

The typical hydrogen feed in a liquefaction plant contains impurities ranging from 10 to 100 ppm [6,24], requiring reduction to below 1 ppm, since they pose a risk of condensing and freezing during cryogenic cooling, potentially degrading the ortho-para catalysts inside the heat exchanger [20,24]. To address this, cryogenic adsorber beds are introduced after precooling PFHX to purify the hydrogen feed. The purified hydrogen enters the main cryogenic cooling system, undergoing cooling from 114 to 30 K through catalytic PFHXs (**HX-3** to **HX-7**). In the process modeling, these heat exchangers, filled with ortho-to-para catalyst on the main hydrogen feed-to-product line, are assumed to be sufficiently long for hydrogen spin isomers to convert to the equilibrium state. The cooling capacity required to cool the incoming hydrogen feed and dissipate the extra heat from exothermic ortho-para conversion in these heat exchangers is provided by the cold hydrogen streams flowing within the HP-H_2 Claude refrigeration cycle. After it cools down to 30 K, the hydrogen gas feed is expanded from 20 to 1.85 bar through a JT valve, resulting in the liquefaction of hydrogen. The temperature of the LH_2 at this point is 22.49 K.

In the HP-H_2 Claude refrigeration cycle, high-pressure hydrogen refrigerant undergoes cooling in heat exchangers **HX-2** and **HX-3** to reach 112 K. Beyond this point along the high-pressure line, auxiliary streams are extracted from the primary high-pressure conduit. These streams, expanded to an intermediate pressure through cryogenic turbines to induce temperature reductions, are then introduced into an intermediate pressure gas return line. This line plays a crucial role in providing cooling for **HX-2** to **HX-6**. The remaining high-pressure hydrogen, exiting **HX-6** at approximately 33.2 K, undergoes expansion in a dense-phase turbo-expander followed by a throttling valve,

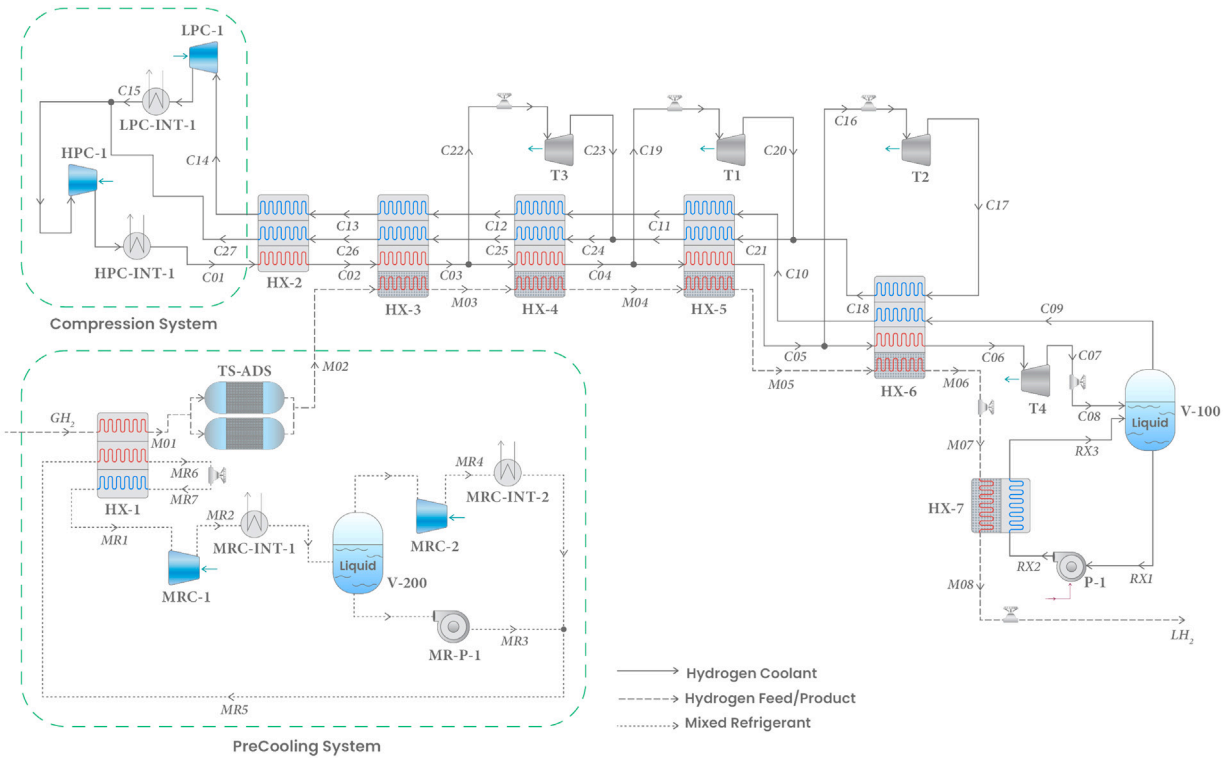

Fig. 1. High-pressure hydrogen Claude cycle hydrogen liquefier process flow diagram.

resulting in a partially condensed hydrogen flow at 21.1 K. The two-phase mixture is directed to a vapor–liquid separator column, where the liquid phase is extracted for use as the cooling source in the final catalytic heat exchanger, **HX-7**. This heat exchanger ensures further cooling and ortho-para conversion of the LH_2 product. The LH_2 stream exits **HX-7** at a temperature of around 21.6 K is further expanded to 1.5 bar for storage and transport. This study considers the LH_2 storage and its boil-off management system to be beyond the battery limit of the liquefaction plant, and, therefore, will not be modeled or further evaluated in the technical and economic analysis.

The collected hydrogen vapors in the vapor–liquid separator are drawn into the low-pressure compressor (LPC), **LPC-1**. The vapor flow passes through all the PFHXs in the main Claude cycle before undergoing compression by the LPC to an intermediate pressure of 7.395 bar. Subsequently, the compressed hydrogen combines with the returning intermediate-pressure stream and undergoes further compression to a pressure of 30 bar, accomplished by the high-pressure compressor (HPC), **HPC-1**. Similar to the MRC units, both the LPC and HPC systems are configured with individual aftercoolers.

Process simulation

The liquefaction process is modeled in the steady-state process simulator of Aspen HYSYS V12. Built-in unit operation models from Aspen HYSYS are used to calculate the process operation of components such as the heat exchangers, commpressors, expanders, etc. For the calculation of the multi-stream counter-current PFHX in the process simulation, Aspen HYSYS's built-in "LNG exchanger" model is used.

In the initial modeling of the liquefaction plant within the process simulation, the efficiencies of the pressure-altering equipment are taken as assumptions. Isentropic efficiencies of 85% are assumed for all compressors and cryogenic turbo-expanders, with a 75% isentropic efficiency assigned to condensate pumps. These efficiency values are refined with the outcomes of the equipment preliminary designs. Similarly, initially assumed negligible pressure drops related to adsorbers and heat exchangers are adjusted and reintroduced into the simulation after the preliminary designs of these components.

The process simulation model employs different fluid property packages according to the respective fluids. As Aspen HYSYS is capable of calling REFPROP databank [25], the thermodynamic properties estimation for the hydrogen refrigerant in the HP-H_2 Claude cycle are calculated using the state-of-the-art equation of state (EOS) of Leachman et al. [26] The hydrogen feed-to-product stream that is cooled in the heat exchangers with continuous catalytic ortho- to para-hydrogen conversion are modeled in the process simulation assuming equilibrium-hydrogen. For this purpose, the "pseudo-equilibrium-hydrogen" heat-capacity model developed by Valenti et al. [27] is utilized. Although the model has faced some criticism in recent literature [28], it has been demonstrated to be a helpful tool for accurately modeling heat exchanger unit operations in hydrogen liquefaction simulations [6,20]. The kinetic aspects of the conversion is only considered in the heat exchanger sizing and preliminary design phase.

In this work, the pseudo-equilibrium model is utilized to calculate the properties of the main GH_2 feed from the exits of the adsorption systems to the final LH_2 product. The pseudo-equilibrium model by Valenti et al. [27] is implemented by modifying the original REFPROP fluid file of parahydrogen and subsequently calling the modified parahydrogen model from Aspen HYSYS. The properties of the MR fluid in the precooling cycle are calculated using the Peng-Robinson cubic EOS.

The author acknowledges that utilizing the pseudo-equilibrium model directly on the hydrogen feed stream at the entrance of the Claude refrigeration cycle may neglect the additional heat from the isomers conversion, stemming from the hydrogen's temperature drop from 298.15 K to 114 K. However, this exothermic conversion yields a modest amount of heat, approximately 57.24 kJ/kg_{H_2}, compared to the total heat removal requirement of around 4432.75 kJ/kg_{H_2} to liquefy hydrogen from ambient temperature (in para-H_2 state). Therefore, it can be concluded that the influence of this conversion on the plant's energy consumption remains marginal.

Table 2
Design limitations of plate-fin heat exchangers [2,20,29,30].

Parameter	Values	Unit
Max. length	8.2	m
Max. width	1.5	m
Max. height	3.0	m
Volume	15–30	m^3
Specific surface	500–1,800	m^2/m^3
Max. temperature difference	25.0	K
Min. temperature difference	1.0	K

3. Equipment preliminary design

Plate-fin heat exchangers

Table 2 summarizes the design constraints assumed for the PFHX, derived based on current equipment limitations found in the literature [2,20,29,30]. If the heat transfer requirement cannot be fulfilled in a single unit while meeting the design constraints, parallel configuration of multiple PFHXs shall be considered. However, the number of cores that can be added is limited by the maximum feasible dimensions of the coldboxes.

Preliminary sizing and design of the non-catalytic PFHXs, **HX-1** and **HX-2**, is performed in Aspen Exchanger Design and Rating (EDR) *design mode*. *Design mode* conducts various calculations of geometric (mechanical), thermal, and hydraulic parameters. It also estimates stream properties and wall temperature for each calculation node, enabling verification of temperature differences against PFHX design constraints. The input for the design is imported directly from Aspen HYSYS simulation of the Claude liquefier described previously. Additionally, pressure drops for each stream within the PFHX are estimated and used to refine the pressure values in the Aspen HYSYS simulation. For noncatalytic PFHXs, the key outcomes of preliminary designs are the Aspen EDR *Design mode* calculation results that align with the criteria specified in Table 2.

For PFHX involving ortho- to para-hydrogen conversion the above sizing procedure is insufficient, since conversion kinetics is the limiting factor in the design. Consequently, this study utilizes the steady-state one-dimensional pseudo-homogeneous continuum reactor model of the counter-flow catalyst-filled PFHX model from O'Neil et al. [31] to approximate the geometric specifications for the catalytic PFHX. This model accounts for the dynamic processes of hydrogen spin-isomer conversion, heat transfer, and pressure loss that occur in a two-stream plate-fin heat exchanger filled with ortho-para catalyst in the hot-stream channel [31]. However, as the catalytic heat exchangers in the liquefaction process simulation are multi-stream models featuring two cold and two hot streams, the preliminary sizing of the multistream catalytic PFHX in this study is divided into two distinct processes:

1. the noncatalytic heat exchanger sizing;
2. the catalytic heat exchanger sizing.

Fig. 2 illustrates the process of splitting the four-stream PFHX, **HX-3**, into a hypothetical three-stream noncatalytic PFHX (with one cold stream and two hot streams), **HX-A**, and a hypothetical two-stream counter-flow catalytic PFHX (a pair of cold and hot streams), **HX-B**. The detailed description of this sizing approach is outlined step-by-step in Section S.1.1 of the Supplementary Information. This catalytic PFHX sizing procedure is applied for the preliminary sizing of **HX-3** to **HX-6**. However, the preliminary design of **HX-7** does not involve the use of the kinetic simulation tool. This is due to the negligible impact of ortho-para conversion on the sizing of **HX-7**, where isomer conversion is less than 1% of its overall composition, resulting in inconsequential conversion time and heat release. Hence, the preliminary sizing and design of **HX-7** are straightforwardly conducted in Aspen EDR *design mode*, following a similar approach as for noncatalytic PFHXs.

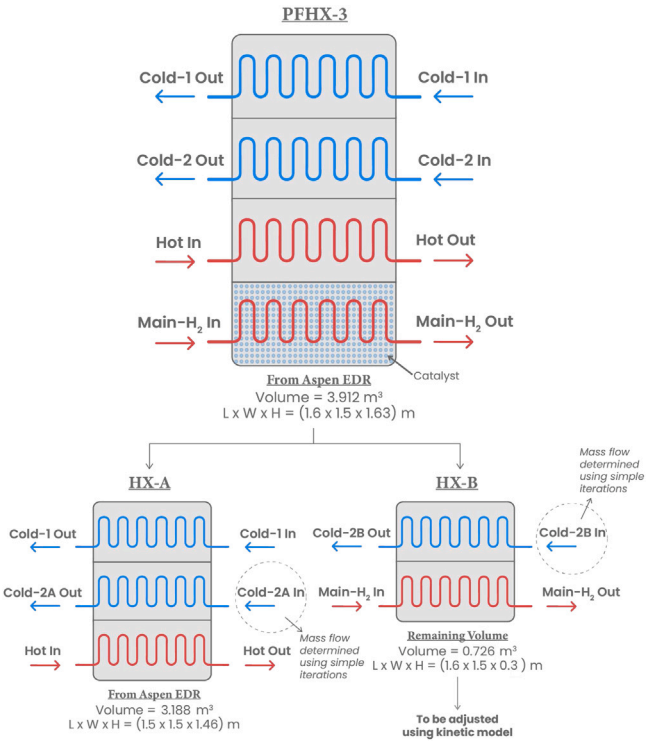

Fig. 2. Schematic for dividing the sizing process of HX-3 into two sizing procedure of noncatalytic and catalytic PFHXs.

The sizing of the catalytic PFHX depends heavily on the evaluation of the streams temperature profiles and conversion of hydrogen spin-isomers across the hot-stream channel of the hypothetical two-stream catalytic PFHX (**HX-B** in Fig. 2). Additionally, the kinetic model simulation computes pressure drop across the catalytic PFHX, and these results are used to adjust the pressure values of the equilibrium hydrogen stream in the process simulation. Conversely, pressure drops for the hydrogen cooling streams are approximated based on the results of the initial sizing of the catalytic PFHX in Aspen EDR.

Given the complexity of the process and equipment, the preliminary design of catalytic PFHXs in this study focuses solely on determining the required core dimensions. The developed procedure ensures that the PFHX designs are sufficiently large for effective heat transfer and hydrogen spin-isomer equilibrium conversion, while meeting dimensional and temperature constraints. These geometric parameters are adequate for making sound cost estimations through APEA. The design algorithm's source code is available in Section 6 and preliminary design results for all PFHXs in the Claude liquefier are given in Section 6.

Turbomachinery

The turbomachinery components within the HP-H_2 Claude liquefier mentioned above include centrifugal compressors and radial inflow turbines. All compression unit operations in the Claude and precooling cycles operate with inlet volumetric flowrates ranging from 4000 to 85,000 m^3/h and a maximum discharge pressure of 30 bar, falling within the optimal range for centrifugal compressors as indicated by Towler & Sinott [32]. Thus, centrifugal compressors are considered the most suitable choice. Additionally, radial inflow turbines are selected, being the type generally specified for turbo-expanders in air separation and petrochemical processes [33,34].

In this study, the preliminary design of these components primarily refers to the comprehensive approach proposed by Gambini & Velinni [35–37]. To ensure the technical feasibility of the outcomes, the

Table 3
Design limitations of centrifugal compressors and radial inflow turbines [4,20,33,38–44].

Parameter	Compressor	Turbine	Unit
Max. Number of stages per unit	8	1	stages
Min. Volumetric inlet flowrates	1000	8.5	m^3/h
Max. Volumetric inlet flowrates	300,000	339,800	m^3/h
Max. Rotational speed	–	100,000	rpm
Max. Power	37,000	1,500	kW
Max. Impeller tip velocity	500	500	m/s

study strictly follows design constraints of centrifugal compressors and radial turbines, given in Table 3, derived in accordance with existing technological limitations within the industry [4,20,33,38–44].

The design procedures for compressors and turbines are identical, with minor differences, and it commences with the process of determining the required number of compression or expansion stages to achieve the required pressure ratio. For hydrogen, the minimum number of stages that can be selected is limited by the compressor's or turbine's maximum impeller tip velocity. To calculate the minimum number of stages, the maximum enthalpy change per stage needs to be determined. For compressors, the following equation is used:

$$\Delta h^{\text{stage}}_{\text{is, max}} = \psi_{\text{is}} \cdot u^2_{2,\text{ max}}. \tag{1}$$

The isentropic work coefficient, ψ_{is}, is assumed to be 0.45, in order to maximize the polytropic efficiency of the centrifugal compressor [36]. For turbines, the following equation is used:

$$\Delta h^{\text{stage}}_{\text{is, max}} = \frac{(u_{1,\text{ max}}/v_s)^2}{2}. \tag{2}$$

The isentropic velocity ratio, v_s, defined as:

$$v_s = \frac{u_1}{c_{\text{is}}}, \tag{3}$$

is assumed to be 0.7, in order to maximize the *total-to-static* efficiency of the radial turbine [36].

Once the maximum isentropic enthalpy change per stage has been determined, one can estimate the minimum number of stages as follows:

$$z_{\min} = \text{Round}\left(\frac{\Delta h_{\text{is}}}{\Delta h^{\text{stage}}_{\text{is, max}}}\right). \tag{4}$$

Note that in Eq. (4), the minimum value is rounded to the nearest integer since the stipulations of $\psi_{\text{is}} = 0.45$ and $v_s = 0.7$ serves only for approximating the required number of stages. The minimum number of stages per component must be below the maximum specified in Table 3. If the minimum number of stages per compressor exceeds the maximum, multiple turbomachinery units in series configuration are considered.

Once the minimum number of stages is determined, we generate the rotational speed and number of stages $(n - z)$ selection diagram. This diagram depicts the turbomachinery's specific speed as a function of the number of stages across varying rotational speeds. The specific speed is defined as follows:

$$\omega_s = f(n, z) = \omega \frac{\dot{V}^{1/2}}{\dot{W}^{3/4}} = \frac{2\pi n}{60} \frac{\dot{V}^{1/2}}{(\Delta h_{\text{is}}/z)^{3/4}}. \tag{5}$$

For a compressor, $\dot{V}$ refers to the volume flowrate at the stage inlet, while for a turbine, it refers to the stage outlet. Fig. 3 shows an example of a compressor's $n - z$ selection diagram. The light blue shaded area represents centrifugal compressor's specific speed range for optimum efficiency.

To ensure high efficiency, the initial number of stages and rotational speed of each compressor and turbine need to be selected such that the specific speed lies in the optimal efficiency range. For centrifugal compressors, this would correspond to specific speed values between

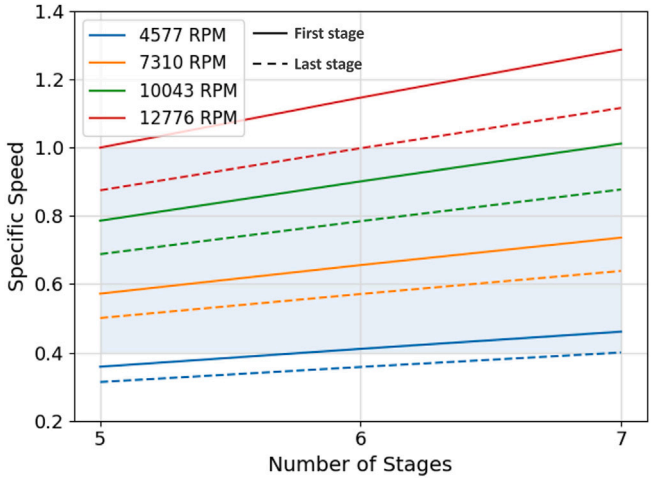

Fig. 3. Exemplary of n-z selection diagram for compressors.

Table 4
Parameter constraints of centrifugal compressors and radial inflow turbines [36,37].

Parameter	Compressor	Turbine
Specific speed, ω_s	0.40–1.00	0.40–0.80
Flow coefficient, ϕ	0.20–0.30	0.20–0.30
Work coefficient, ψ	0.50–0.60	0.80–1.00
Degree of reaction, R	0.60–0.70	0.45–0.65
Rotor meridional velocity ratio, ξ	–	0.65–1.00
Rotor tip diameter ratio, δ_t	0.50–0.75	<0.70
δ_t/δ_h	0.20–0.70	> 0.40
Rotor outlet absolute flow angle, α_2	60°–70°	–
Rotor outlet relative flow angle, β_2	0°–60°	–
Rotor inlet absolute flow angle, α_1	–	66°–78°
Rotor inlet relative flow angle, β_1	–	22°–40°
Impeller tip speed velocity, u	<500 m/s	<500 m/s
Mach number, Ma	<0.90	<0.90

$0.4 \leq \omega_s \leq 1$ [36]. For radial inflow turbines, this range is between $0.4 \leq \omega_s \leq 0.8$ [37].

The initial values for the number of stages and rotational speed serve as the primary inputs for calculating kinematic, thermodynamic, and geometric parameters of components, including work coefficient, flow coefficient, flow angles, blade height, rotor diameter, etc. In this study we developed a simplified version of the design calculation procedure proposed by Gambini & Vellini [36,37]. This simplification involves omitting stage losses evaluation, with turbo-component efficiencies estimated based on existing correlations. The results of kinematic, thermodynamic, and geometry calculations undergo an iterative process of comparison with constraints proposed by Gambini & Vellini [36,37]. The preliminary design of centrifugal compressors and radial inflow turbines is deemed acceptable when the calculated parameters align with design constraints throughout all stage calculations. Parameter constraints assumed for the preliminary design of multistage centrifugal compressors and radial turbines are summarized in Table 4.

The complete procedure and assumptions for turbomachinery preliminary design are given in Section S.1.2 and S.1.3 of the Supplementary Information. The source codes implementing the proposed design algorithms are accessible in the GitHub repository provided in Section 6. The preliminary design results for all turbomachinery components are provided in Section 6.

Cryogenic adsorbers

Temperature-swing adsorbers (TSA) are selected as the cryogenic adsorption system in the hydrogen liquefaction process in this study. The preliminary design of the TSA focuses on estimating the required

size and number of adsorber columns, which are crucial parameters for sizing the precooling coldbox and estimating costs related to the adsorption system.

To determine the required dimensions (diameter and height) and number of columns of the adsorption system, we have used the sizing algorithm based on the design procedure described by Campbell [45]. The regeneration process of the adsorbers is expected to utilize a portion of the hot hydrogen streams from the Claude cycle as the high-temperature source. However, the evaluation of this process is not covered in this study.

Coldbox

The preliminary coldbox design aims to adequately size the MR precooling and cryogenic liquefier coldboxes to accommodate components operating in cryogenic conditions. These components include adsorption columns, PFHXs, turbo-expanders, vapor–liquid separators, and cryogenic pumps.

In addition to the cryogenic equipment, it is important to account for the space required by piping and auxiliary process items, including valves and control devices. To ensure sufficient space for these components, a clearance of 1.3 is applied to the estimated volumes of the PFHXs and separator columns. The estimated volumes of the turbo-expanders, whether in single or multiple configurations, have already considered the space needed for their connections and instrumentation. The approximated footprints of the turbo-expander systems, available in Section S.1.4 of the Supplementary Information, are based on turbine brochures from various manufacturers.

An additional clearance of 10% is incorporated into the total volume of the internal components, including their own clearances, to accommodate the coldbox's wall thickness and insulation material. In this study, both the precooling and liquefier coldboxes are assumed to have a capsule-like structure (spherocylinder), a three-dimensional shape comprising a cylinder with hemispherical ends. The main geometrical parameters of the vessel are the radius and the height of the cylinder. After determining the required volume of the vessel, optimized radius and height values are obtained using Microsoft Excel's GRG Nonlinear Solver. Since vacuum-insulated coldbox is generally prefabricated off-site, the radius and height of the liquefier coldbox are limited to 5.5 and 40 m, respectively, in order to comply with the typical logistical limitation within Europe [20,46].

4. Techno-economic analysis

Techno-economic analysis (TEA) is a method used to evaluate the economic performance of a technology. In this study, TEA is performed to assess the overall value of the conceptual plant described previously, enabling analysts to objectively weigh the benefits of LH_2 against the cost of the large-scale Claude-cycle liquefaction process. The primary objective in this TEA is to compute the SLC, defined as follows:

$$\mathrm{SLC} = \frac{\mathrm{CAPEX_a} + \mathrm{OPEX_a}}{\dot{m}_{\mathrm{LH_2},a}}. \tag{6}$$

The capital and operating expenditures are determined using APEA software, selected for its capability to estimate equipment expenses based on recent cost data from EPC projects and equipment manufacturers from limited design data [47,48]. APEA calculates the equipment costs as well as the total installed costs, covering both direct and indirect field costs for capital expenditure (CAPEX) evaluation. In this study, we employ APEA V12, which estimates equipment costs based on pricing updates from the 1st Quarter of 2019. These estimates are then adjusted to reflect 2022 pricing using the Chemical Engineering Plant Cost Index (CEPCI).

Another notable advantage of APEA, compared to other methodologies, is its integration with Aspen HYSYS software used for process modeling in this study. The cost estimation for the main equipment relies on unit operation models from Aspen HYSYS simulation, which are then mapped into component models within APEA and further specified with design parameters derived from preliminary design results. APEA offers the convenience of providing cost estimates with relatively few inputs for preliminary studies. However, it is crucial to note that these type of estimates, especially for the equipment capital costs, are classified as "Class 4" estimates [49]. This type of estimate has an accuracy range of ± 30%, making it more suitable for comparing costs among process concepts rather than for making investment decisions.

To determine the plant's CAPEX annual cost contribution, this study considers the total project capital cost as a fixed annuity payment. The subsequent formula for capital recovery factor is then utilized to determine the annual CAPEX:

$$\mathrm{CAPEX_a} = \mathrm{CAPEX_{tot}} \cdot \frac{I_{\mathrm{fix}} \cdot (1 + I_{\mathrm{fix}})^{t_p}}{(1 + I_{\mathrm{fix}})^{t_p} - 1}. \tag{7}$$

The fixed annual interest rate is typically assumed between 0.07 and 0.11, as reported by Syed et al. [50]. In this study, a payment duration of 20 years is assumed.

Additionally, APEA facilitates the calculation of the plant's variable and fixed operating expenditures (OPEX) on a yearly basis. This figure is further adjusted to account for the cost contribution of fluid loss due to expected leaks from turbomachinery components. Hydrogen leaks are assumed to constitute 1.5% of the plant's capacity, while the cost of hydrogen itself is presumed to be €3.5/kg_{H_2}. For a liquefier capacity of 125 TPD, the makeup flow required to compensate for MR leaks is assumed to amount to 1.5 kg/h, with a specific cost of €5.0/kg_{MR}.

The TEA workflow and assumptions used in this study are given in Section S.2 of the Supplementary Information. This includes the **Project Basis** that defines specifications pertaining to the overall project scenario. The complete list of equipment cost parameters are also included in this section.

5. Results and discussions

Baseline scenario

Fig. 4 illustrates the preliminary design results of the compression system of the 125 TPD HP-H_2 Claude-cycle, featuring substantial modifications from the initial configuration in Fig. 1. The additional turbocompressors became necessary due to design constraints, shown in Tables 3 and 4, in the equipment preliminary design, which limits the maximum allowable compression ratios within a single compressor unit. In the LPC system, three separate units (**LPC-1**, **LPC-2**, and **LPC-3**) are employed, each with eight radial compression stages and isentropic efficiencies of 83.03%, 82.45%, and 82.66%, respectively. The HPC system features **HPC-1**, **HPC-2**, and **HPC-3**, each with six radial compression stages and isentropic efficiencies of 83.26%, 82.95%, and 82.93%, respectively. The MRC system, **MR-1** and **MR-2**, maintain the original configuration and are designed as two-stage and single-stage centrifugal compressors with isentropic efficiencies of 83.33% and 83.00%, respectively. The number of stages are selected in conjunction with the rotational speeds through iterative trials for high performance while meeting the design constraints.

The preliminary design of the turbo-expanders calls for two expansion stages between Stream *C22* and *C23*. As a result, turbo-expander **T-3** are split into **T-3A** and **T-3B**, arranged in series to achieve the required expansion ratio. The isentropic efficiencies for **T-1**, **T-2**, **T-3A**, **T-3B**, and **T-4**, are calculated as 89.68%, 89.53%, 87.90%, 90.50%, and 89.34%, respectively. Furthermore, the pressure losses identified during the preliminary designs of the TSA and PFHXs are reintroduced into the process simulation of the final plant configuration. Streams data for the HP-H_2 Claude liquefier, following the equipment preliminary design results, is summarized in Table 5.

In this scenario, the plant's overall SEC is determined to be 7.241 kWh/kg_{LH_2}. If turbo-generator systems are considered to recover the

Table 5
Stream data of the refined HP-H_2 Claude cycle hydrogen liquefaction process.

Stream[a]	Temp. [K]	Press. [bar]	Flowrate [kg/h]	Vapor quality	Stream[a]	Temp. [K]	Press. [bar]	Flowrate [kg/h]	Vapor quality
Hydrogen refrigerant streams									
C01	298.1	29.80	51,498.8	1	*C16*	47.4	29.44	16,662.1	1
C02	119.4	29.705	51,498.8	1	*C17*	29.89	7.895	16,662.1	0.9942
C03	112.0	29.607	51,498.8	1	*C18*	44.36	7.797	16,662.1	1
C04	74.0	29.522	34,504.2	1	*C19*	74.0	29.522	15,527.0	1
C05	47.4	29.440	18,977.3	1	*C20*	46.0	7.797	15,527.0	1
C06	33.20	29.391	2,315.2	1	*C21*	45.2	7.797	32,189.0	1
C07	25.41	3.500	2,315.2	0.1939	*C22*	112.0	29.606	16,994.6	1
C08	21.1	1.250	2,315.2	0.2936	*C23*	71.2	7.699	16,994.6	1
C09	21.1	1.250	2,315.2	1	*C24*	70.47	7.699	49,183.6	1
C10	25.1	1.244	2,315.2	1	*C25*	102.4	7.599	49,183.6	1
C11	71.9	1.197	2,315.2	1	*C26*	111.3	7.501	49,183.6	1
C12	111.0	1.151	2,315.2	1	*C27*	293.6	7.401	49,183.6	1
C13	118.4	1.107	2,315.2	1	*RX1*	21.10	1.250	1,609.1	0
C14	297.1	1.059	2,315.2	1	*RX2*	21.10	1.251	1,609.1	0
C15	298.1	7.401	2,315.2	1	*RX3*	21.70	1.250	1,609.1	1
Hydrogen feed to product streams					Mixed refrigerant streams				
GH_2	298.1	20.00	5,208.0	1	*MR1*	292.0	3.451	72,000.1	1
M01	114.0	19.923	5,208.0	1	*MR2*	298.1	12.066	72,000.1	1
M02	114.0	19.778	5,208.0	1	*MR3*	300.0	35.000	11,381.5	0
M03	106.0	19.647	5,208.0	1	*MR4*	298.1	35.000	60,618.6	0.7437
M04	73.5	19.618	5,208.0	1	*MR5*	300.1	35.000	72,000.1	0.6444
M05	46.0	19.555	5,208.0	1	*MR6*	114.0	34.851	72,000.1	0
M06	30.0	19.544	5,208.0	1	*MR7*	111.3	3.600	72,000.1	0.0689
M07	22.49	1.850	5,208.0	0.2992					
M08	21.60	1.849	5,208.0	0					
LH_2	21.63	1.500	5,208.0	0					

[a] Stream names refers to Fig. 1.

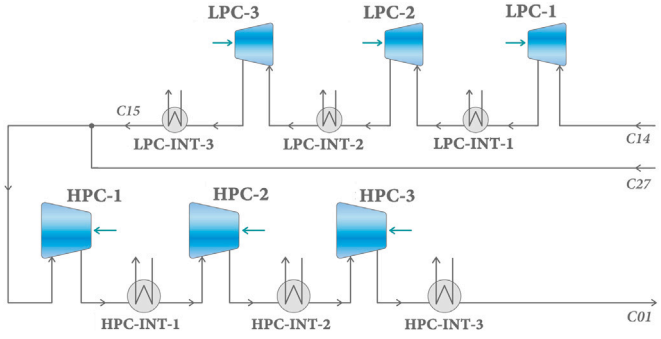

Fig. 4. The refined PFD of the Claude-cycle compression system based on compressors preliminary design results.

mechanical power from the turbines, assuming mechanical to electrical energy conversion efficiency of 80%, the plant's SEC would further decreases to 6.666 kWh/kg_{LH_2}. Among the plant major systems (cryogenic liquefaction, compression, and precooling), hydrogen compression system emerges as the largest contributor to the total plant SEC, accounting for 6.478 kWh/kg_{LH_2}.

We would also like to highlight the importance of using a hydrogen model that accounts for the exothermic heat from ortho-to-para conversion in the process simulation, as this can markedly affect the plant's SEC calculation. Without incorporating the 'pseudo-equilibrium-hydrogen' model, the simulations yield an SEC of 6.299 kWh/kg_{LH_2} without power recovery and 5.807 kWh/kg_{LH_2} with power recovery, which are about 13% lower than when considering the isomer conversion. As will be shown later in this section, the plant's OPEX greatly influences annual costs, thus ignoring the conversion can substantially skew the SLC predictions.

Further calculations reveal that the ideal specific work of the concept is 2.857 kWh/kg, inclusive of the ortho- to para-hydrogen conversion. Based on this finding, the baseline scenario's exergy efficiency is 39.45%, increasing to 42.85% when power recovery is considered.

Table 6
Base scenario assumptions of plant, equipment and TEA parameters.

Plant and equipment design parameters	Values	Unit
Plant liquefaction capacity	125	TPD
Compressor max. impeller tip velocity	500	m/s
H_2 leakage rate	78.13	kg/h
MR leakage rate	1.5	kg/h
TEA (APEA) parameters		
Process description	New process	
Fixed annual interest rate	0.09	
Electricity cost	0.1	€/kWh

Table 6 provides a list of parameter assumptions established for the SLC computations in the baseline scenario. Unless explicitly stated otherwise in subsequent analyses, the parameters remain consistent with the values specified in this table. The plant's cost estimation in this scenario yields an SLC of €1.55/kg_{LH_2}, decreasing to €1.51/kg_{LH_2} when considering the implementation of power recovery systems.

Table 7 summarizes the number of parallel units, main cost-parameters, and direct costs for the primary equipment of the liquefaction plant (without power recovery systems). Notably, the direct costs of the hydrogen compression system, consisting HPCs and LPCs, constitute a significant portion, accounting for €51 million within the overall project capital of about €154 million (in 2019 pricing). This aligns with the observation of Essler et al. [46] that compression systems can readily constitute 50% of total equipment investment for hydrogen liquefiers.

Fig. 5 shows the distribution percentage of base scenario annual OPEX. The estimated annual OPEX is approximately €43 million after accounting for fluid losses. The utility expenses, mainly electricity, comprising a significant portion of €33.3 million annually. The annual OPEX ratio relative to the annual CAPEX is approximately 1.79:1.00.

The SEC values of the large-scale liquefaction process outlined in this study are significantly lower than those reported for state-of-the-art hydrogen liquefiers, typically ranging between 10–12 kWh/kg_{LH_2}. As previously noted, the annual OPEX of the plant contributes almost

Table 7
Equipment main cost-parameters and direct costs for baseline scenario.

Equipment	Parallel units	Parameter 1	Parameter 2	Total direct costs[a]
Compressors		Inlet flowrate [m^3/h]	Power input [kW]	
LPC-1	1	29,480.1	676.7	€6,057,300
LPC-2	1	15,482.8	682.0	€3,214,800
LPC-3	1	8,107.1	682.4	€1,712,400
HPC-1	1	93,142.7	10,397.5	€18,310,900
HPC-2	1	59,564.9	10,622.7	€10,771,300
HPC-3	1	37,594.6	10,675.7	€8,910,700
MRC-1	1	16,201.3	2,293.8	€2,338,900
MRC-2	1	4,006.3	1,663.8	€1,574,600
Turbines		Inlet flowrate [m^3/h]	Power output [kW]	
T-1	1	1,689.2	1,127.2	€853,900
T-2	1	883.7	552.2	€563,600
T-3A	1	2,950.8	1,003.3	€942,900
T-3B	1	4,311.7	1,064.3	€822,200
T-4	1	44.7	30.8	€300,200
PFHXs		Dimensions [m]	Core weight [kg]	
HX-1	1	(6.1 × 1.5 × 1.8)	18,411.5	€1,630,300
HX-2	2	(4.4 × 1.5 × 2.9)	17,910.7	€2,702,500
HX-3	1	(4.0 × 1.5 × 3.0)	–	€1,675,600
HX-4	2	(4.8 × 1.5 × 2.5)	–	€3,330,100
HX-5	1	(7.7 × 1.5 × 2.9)	–	€2,603,400
HX-6	1	(6.0 × 1.5 × 3.0)	–	€2,381,700
HX-7	1	(1.6 × 1.0 × 1.0)	17,910.7	€367,700
Coldboxes		Dimensions [m]	Tan-tan height [m]	
Precooling	1	2.37	7.12	€547,000
Cyogenic	1	4.68	18.22	€1,620,300

[a] Estimated based on APEA 2019 pricing.

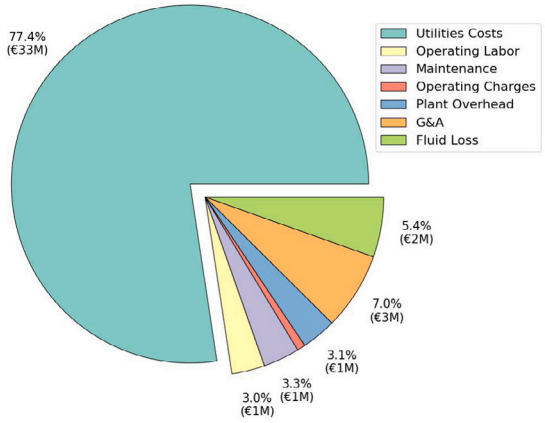

Fig. 5. Distribution percentage of base scenario annual OPEX.

twice as much to the SLC as the annual CAPEX of the plant. Therefore, it can be inferred that the relatively modest SEC values of the conceptual plant serve as the primary driver for the significantly reduced SLC values, in comparison to reported figures for existing hydrogen liquefiers ranging from €2.37 to €2.85 per kg_{LH_2}.[1]

Another contributing factor to the cost improvement is the economy of scale achieved by the plant. Larger liquefaction facilities typically demonstrate lower construction costs per unit of liquefied gas. Towler & Sinnott [49] note that gas compressors, identified as the most expensive components in capital cost estimation, exhibit cost-scaling exponents of 0.6 and 0.75 for reciprocating and centrifugal types, respectively. This implies that the specific purchased cost of compressors decreases with increasing compressor capacity. Given the substantial scale-up in capacity of the conceptual plant compared to existing hydrogen liquefiers, it is plausible that the cost curve of compressors significantly contributes to the enhanced SLC outcome.

Electricity cost sensitivity

In this sensitivity analysis, the total annual costs and SLC of the 125 TPD conceptual plant are computed for varying electricity costs between €0.02 and €3.0 per kWh. The results are presented in the right graph of Fig. 6. Meanwhile, the left graph in the same figure illustrates the estimated overall capital expenses of the plant. Both charts are plotted with the same costs axis (left y-axis) for comparison.

The graphs highlight the considerable influence of electricity costs on the SLC of the liquefier. The SLC increases to the current industrial range of €2.37 to €2.85 per kg_{LH_2} when electricity is priced relatively high at €0.20 to €0.25 per kWh. With electricity price of €0.4/kWh, the plant's total annual expenses reach essentially €175 million, a figure which corresponds to 80% of the entire project CAPEX. Conversely, when the electricity price is €0.05/kWh the SLC rapidly decrease to an optimistic value suggested in literature, approaching €0.95/kg_{LH_2}. In recent years, the expenses associated with wind power generation have fallen and are projected to continue decreasing to about €0.02/kWh [51]. If such low-cost sources were harnessed for liquefaction, the SLC might even be less than €0.90/kg_{LH_2}. Additionally, the range of electricity prices in this analysis is deliberately chosen to exceed the typical variation of electricity costs in the European Union (EU), aiming to demonstrate the impact of a sudden surge in energy prices, similar to what the EU has witnessed in recent years,[2] on the overall costs of the hydrogen supply chain.

Furthermore, it is apparent that the OPEX contribution to the SLC becomes very dominant at high electricity price. In fact, when the electricity price is doubled from the baseline value, the annual OPEX is four times higher than the annual CAPEX. As OPEX increases, the economic benefit of incorporating recovery generators becomes more pronounced. However, this improvement is negligible compared to the drawbacks that the plant would face at high electricity price.

Feed pressure analysis

As highlighted by Berstad et al. [6,53], the ideal energy input required for a hydrogen liquefaction process decreases as the hydrogen feed pressure increases. Therefore, the efficiency the process is more favorable in plants with higher hydrogen feed pressures. In this analysis, the plant's SEC and SLC are computed for hydrogen feed pressures of 1, 5, 10 and 20 bar to evaluate the plant feasibility when using lower feed pressures.

To assess lower hydrogen feed pressures, this study considers a feed precompression system to increase the pressure to 20 bar before the precooling system. This approach is chosen instead of adjusting the stream conditions of the plant, as it is challenging to perform a consistent sensitivity analysis with stream adjustments without an optimization procedure. The precompression system consists of one or multiple centrifugal compressors with aftercoolers, designed according to . The configuration of the precompression systems and outcomes of SEC and SLC calculations for each feed pressures are shown in Fig. S.15 and S.16 in the Supplementary Information, respectively.

This analysis demonstrates that the efficiency and economic performance of the plant design are sensitive to reductions in hydrogen feed pressure. While feed pressure significantly affects the SLC, it is less substantial compared to the effect of variations in electricity costs.

[1] Converted from 2.5–3.0 US Dollar per kg_{LH_2} using 2022 average exchange rate of €1 = US$1.053. Sourced from www.ecb.europa.eu, accessed on 28 August 2023.

[2] During this research, the EU faced a record annual energy inflation exceeding 40% in June 2022 due to the ongoing conflict in Europe. The wholesale electricity price peaked at €0.82/kWh and gradually decreasing afterward [52].

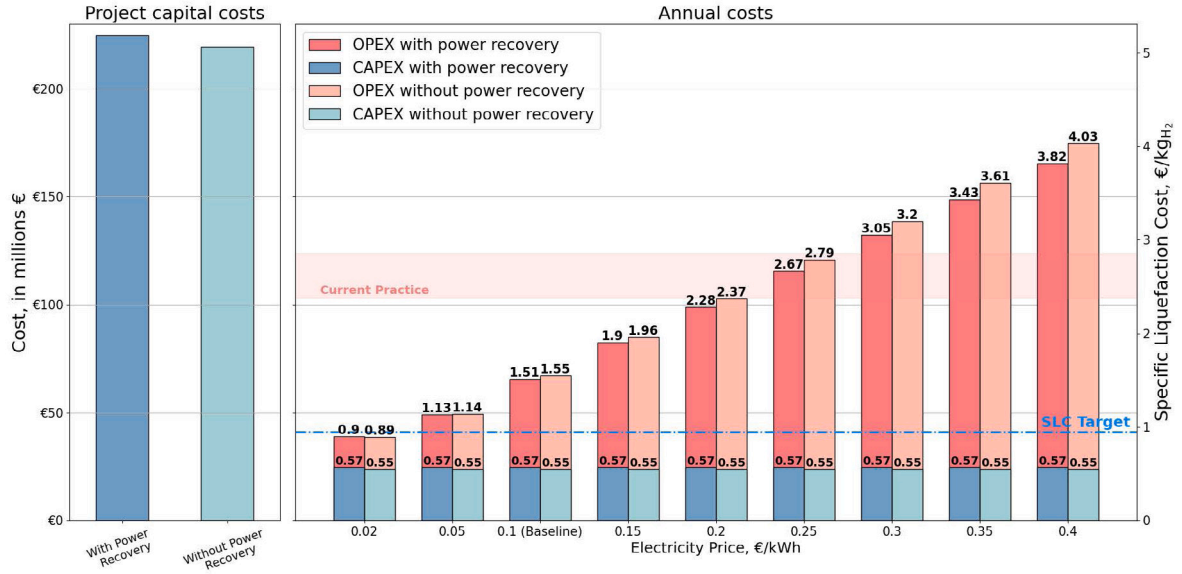

Fig. 6. SLC of the 125 TPD hydrogen liquefier concept as a function of specific electricity costs.

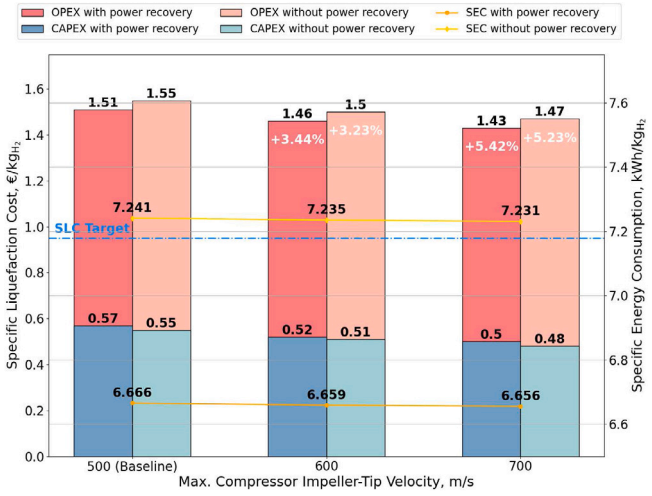

Fig. 7. SEC and SLC of the 125 TPD hydrogen liquefier using different compressor's max. tip velocity.

Compressor's max. Impeller tip speed velocity

Considerable research is currently underway to enable the use of centrifugal compressors for large-scale hydrogen compression [38,54,55]. Many are focused on the development centrifugal compressors capable of operating at higher impeller tip velocities [56–58], aiming to ultimately reduce the required number of stages for a given hydrogen compression. In this analysis, the tip speed limit in the compressor design constraints is varied from the base value of 500 m/s to 600 and 700 m/s.

With an increased maximum tip speed, the design of the plant's compression system becomes more compact, since it reduces the total number of compression stages in both the LPC and HPC units. Since the total number of aftercoolers within the compression system has a significant influence on the performance of the liquefier, to give a more comparable analysis between compression systems, the total number of compressor units, including the aftercoolers, is maintained at three for both LPC and HPC systems. Therefore, only the number of stages in each compressor is reduced as the tip speed limitation increases.

The design results reveal that with a maximum impeller tip velocity of 600 m/s, both LPCs and HPCs experience a reduction of two stages, resulting in a total of 6 and 4 compression stages for each LPC and HPC, respectively. When the maximum tip speed is at 700 m/s, the number of stages in each LPC is further reduced by two, leaving each with 4 compression stages The HPCs see a further reduction of one stage, with each HPC now consisting of 3 compression stages. The corresponding SEC and SLC of the liquefier following these design configurations are displayed in Fig. 7.

The figure illustrates a minimal deviation in the SEC of the plant when examining compression systems with different maximum tip speeds, attributed to the specific speed of compressors, a key parameter for estimating isentropic efficiency in this study, which remains relatively steady across each design. The uniformity in specific speed values stems from design constraints, ensuring that specific speed falls within a comparable range. Notably, the design process occurred without the use of an optimization scheme, raising the possibility that a higher impeller tip speed could potentially yield greater efficiency through a design optimization procedure. The marginal improvement in the SLC primarily results from a reduction in annual CAPEX. According to APEA's cost estimates for compressors, the integration of high-speed compressors is anticipated to boost the SLC by 3.0% to 5.5%. To contextualize, a 5% SLC enhancement in a 125 TPD hydrogen liquefier translates to roughly €3 million in annual savings.

Another important aspect to note is that compressors direct-cost estimation provided by APEA only accounts for the differences in cost associated with the reduced number of stages, changes in power requirements, flowrates, and other process parameters. Thus, this study overlooks the additional expenses related to high-strength materials and advanced manufacturing required for producing high-speed hydrogen compressors. These are likely to increase the equipment's purchase costs beyond APEA's predictions, potentially offsetting any savings gained from fewer compression stages. For more accurate estimation, the projected commercial costs of high-speed hydrogen compressors must first be obtained.

Equipment cost sensitivity

As mentioned in Section 4, the capital cost estimates from APEA in this study have an accuracy range of ±30%. To evaluate the impact of this uncertainty on the SLC calculations, we varied the CAPEX of the 125 TPD liquefaction plant concept from the base scenario by ±30% in

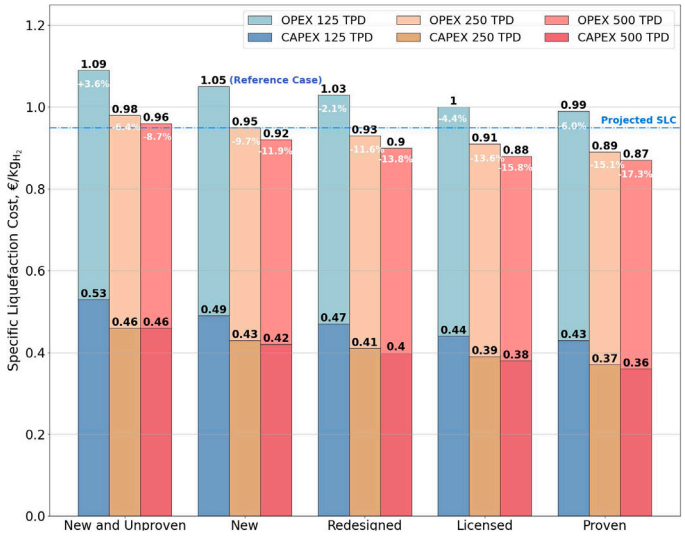

Fig. 8. SLC results for hydrogen liquefiers employing power recovery, with fixed annual interest rate of 0.07 and electricity costs of €0.05/kWh.

5% increments. The results, shown in Fig. S.17 in the Supplementary Information, indicate that the ±30% variation in CAPEX results in an SLC error range of ±10.74% for the baseline scenario. Approximately the same error values are observed in the scale-up scenarios. The error range is expected to decrease at higher electricity prices due to the greater contribution of OPEX to overall annual costs.

Scale-up and best case projection

Leveraging economies of scale, industrial experience, green policies, and renewable infrastructure presents opportunities for cost improvements in the hydrogen supply chain. This analysis focuses on projecting optimal cost reductions for hydrogen liquefaction by considering financial incentives, scale-up effects, reduced design allowances, and access to low-cost electricity.

Low-carbon policies, such as reduced interest rates for large-scale low-carbon fuel production, could improve hydrogen liquefaction costs. To reflect this, the fixed annual interest rate for the plant's annual CAPEX calculation in this analysis is reduced from the base value of 0.09 to 0.07. Additionally, the analysis involves scaling up the 125 TPD liquefaction plant from the base scenario to 250 and 500 TPD plants. This scaling-up process includes readjusting the process simulation, equipment design, and TEA, adopting more and/or larger equipment while maintaining the 125 TPD plant configuration. The SEC of the plant remains essentially constant as the capacity increases,as no alterations were made to the stream data, except for adjustments in mass flowrates and pressure drops.

Looking ahead, as larger hydrogen liquefiers are successfully constructed, the technology is expected to mature, allowing companies to undertake projects with reduced design allowances and project contingency. The analysis explores the impact of varying design allowances and contingencies on SLC by adjusting the APEA "Process Description" input. Table S.4 in the Supplementary Information illustrates the changes in design allowances and contingency percentages employed by APEA based on different selections of "Process Description".

Fig. 8 presents the results of SLC calculations for liquefaction plants with capacities of 125, 250, and 500 TPD under different 'Process Description' selections. The calculations assume a relatively low specific electricity price of €0.05/kWh and the implementation of turbine power-recovery systems. The figure indicates that, with relatively modest project interest rates and electricity costs, large-scale Claude-cycle hydrogen liquefiers have the potential to substantially reduce the industrial liquefaction cost of hydrogen to around €1.0/kg$_{LH_2}$. This aligns

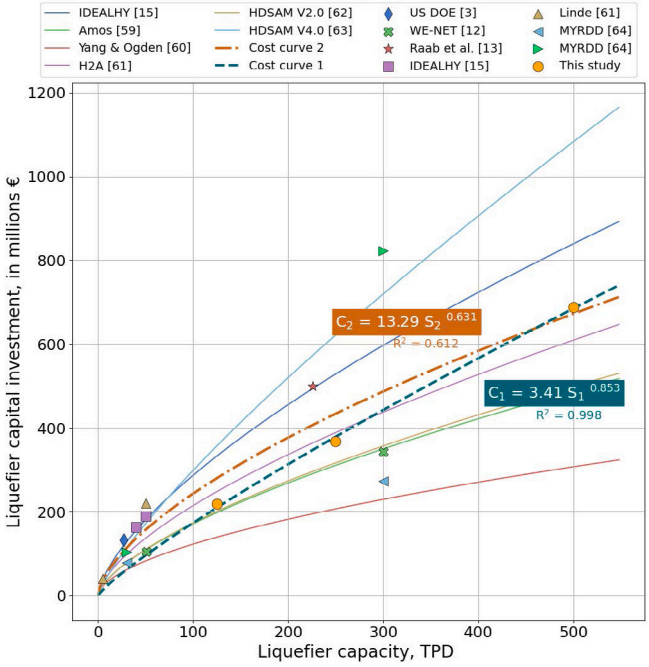

Fig. 9. The cost curves and capital cost data from this study and those found in the literature.

with recent cost projection studies discussed in the literature. Moreover, the calculations suggest that as hydrogen liquefaction technology matures within the industry, the SLC for capacities of 250 TPD and 500 TPD could potentially decrease to approximately €0.87/kg$_{LH_2}$.

Further exploration of the SLC results reveals additional insights discussed in Section S.3.3 of the Supplementary Information. In the same section, Table S.5 summarizes the number of parallel units, main cost parameters, and direct costs of the process equipment associated with scaled-up plants.

Cost and experience curves

Numerous cost curve models have been published to estimate the capital investment associated with hydrogen liquefaction plants [15, 59–63]. This section utilizes capital cost estimations from the current

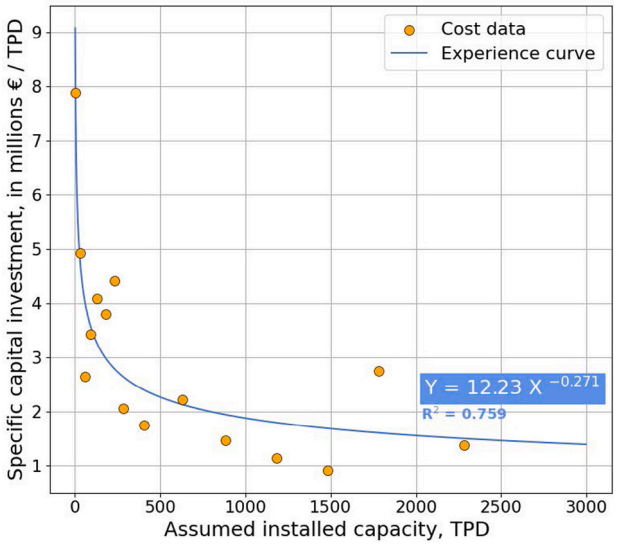

Fig. 10. Prediction of experience curve of hydrogen liquefaction technology based on cost data from this study and those found in the literature.

study to formulate a novel cost curve, denoted as *Cost Curve 1*. The estimations are derived from the APEA process descriptions of "New Process", "Redesigned", and "Licensed" for 125, 250, and 500 TPD concepts, respectively. The resulting curve is juxtaposed with existing cost curves in Fig. 9. Within the same figure, *Cost Curve 2* is introduced, amalgamating capital cost findings from this research with reported costs data stemming from project reports, contractor quotations, and cost projections [3,12,13,15,61,64]. All cost curve models and capital cost data are adjusted to 2022 pricing in € for a more meaningful comparison. Both cost curves are constructed using the following equation [49]:

$$C = \frac{C_0}{S_0^n} \times S^n = mS^n, \tag{8}$$

each yielding distinct constant, m, and capital cost exponent, n, as shown in Fig. 9. As illustrated, both curves fall within an intermediate range compared to values from other models.

Evidently, *Cost Curve 1* predicted a higher scaling coefficient than other models, possibly due to reaching the limit of the economy-of-scale potential of high-pressure centrifugal compressors in the 500 TPD plant (refer to Section S.3.3 of the Supplementary Information). Additionally, existing literature models lack cost data for plants exceeding 300 TPD, which may contribute to the higher scaling coefficient of *Cost Curve 1*. Nevertheless, the study's capital cost results are comparable with estimates from published hydrogen liquefier cost projection models. This asserts the value of the methodologies in process modeling, preliminary design, and TEA developed in this study, affirming their utility in predicting the economic viability of large-scale hydrogen liquefaction processes.

In addition to cost curves, the experience curve for hydrogen liquefaction technology is predicted based on previous capital cost data by rearranging the plant capacities in a cumulative sum array, starting from the smallest capacity and progressing to the largest. The assumption is that all of the referred liquefier concepts have been globally installed in a sequential manner, from the smallest concept to the largest. The manipulated data is then fitted into the experience curve log-linear equation [65]:

$$c = c_0 \left(\frac{q}{q_0}\right)^{-b} = a \cdot q^{-b}. \tag{9}$$

The results are depicted in Fig. 10. The experience curve reveals a constant a of €12.23 million per plant capacity and a learning coefficient b of 0.271, corresponding to a progress ratio and learning rate of 82.87% and 17.13%, respectively. These results mean that with each doubling of the installed global liquefaction capacity the price of hydrogen liquefiers is predicted to drop on average by 17.13% [66]. This is comparable to solar panels, which have learning rate of around 20.20% [67].

Fig. S.18 in the Supplementary Information extends the x-axis of the experience curve to 20,000 TPD, revealing a decrease in specific capital investment up to €0.81 million/TPD. Using the economic assumptions and OPEX contributions from the base scenario, this corresponds to an overall SLC result of €1.28/kg_{LH_2}, marking a 17.66% reduction from the baseline SLC of €1.55/$kgLH_2$. While promising, these findings rely on extrapolation of preliminary cost estimates and capital investment data that are based on varying assumptions and levels of comprehensiveness. In practice, technological constraints may well hinder cost improvements at the above anticipated rate.

6. Concluding remarks & recommendation

This research streamlines the evaluation of large-scale hydrogen liquefier concepts, emphasizing both technical and economic feasibility. It introduces an alternative preliminary equipment design for the HP-H_2 Claude-cycle hydrogen liquefier concept, followed by an economic assessment, contributing valuable insights to the development of cost-scaling curves. The results align with existing cost curves reported by industry and government research collaborations, thereby validating the methodologies developed in this study.

Sensitivity analyses reveal the substantial impact of electricity price changes on the plant's economic performance. The study demonstrates that the SLC for large-scale hydrogen liquefaction can meet the literature-suggested target of US$1/$kg_{LH_2}$, with an electricity cost of approximately €0.05/kWh. However, as mentioned in Section 4, it is important to recognize that the cost estimates in this study are categorized as "Class 4" estimates, with an accuracy range of ± 30%. The inherent uncertainty in these estimates could lead to significantly higher or lower liquefaction costs in the actual implementation of the concept. Despite this, the authors argue that the SLC results likely underestimate liquid hydrogen's true potential for cost-effective hydrogen transportation and storage.

There are two key reasons for this assertion. Firstly, APEA calculates costs assuming liquefaction facilities resemble conventional chemical plants. In reality, hydrogen liquefaction construction significantly differs, with equipment installed in cryogenic coldboxes inside production buildings, resulting in a smaller land footprint. Furthermore, due to the encapsulation of most of the components within the coldbox, the plant operation is likely to be centralized. This has the potential to reduce the number of operating personnel compared to what would be necessary for conventional plants. These aspects can be taken into account by making certain adjustments in APEA, however, more construction and operation data are needed for accuracy.

Secondly, the methodology developed for process modeling and equipment design in this study lacks an optimization component, thereby limiting the achievable efficiency and cost-effectiveness of large-scale hydrogen liquefaction from its true potential. Although the incorporation of optimization steps is desirable, it presents challenges due to the reliance on APEA for capital cost estimation in this framework. Cardella previously conducted liquefaction cost optimization by integrating Honeywell UniSim Process Simulation with Matlab [20], but the cost estimation relied on self-developed correlations that were not fully published. Given the benefits, the authors highly encourage to improve the proposed methodologies with an optimization study for future research. However, before implementing optimization, a more robust preliminary equipment design is deemed essential, particularly for the catalytic PFHXs.

This study integrates Aspen EDR outcomes with the continuum reactor model of O'Neil et al. [31] to estimate the core size for catalytic

PFHX design. This integration is necessary because the PFHX model by O'Neil et al. initially devised for two-stream catalytic PFHXs, lacks direct applicability to the prevalent three- or four-stream PFHX configurations employed in large-scale hydrogen liquefaction. To enhance design robustness, it is highly recommended to develop a dedicated steady-state continuum reactor kinetic model for these configurations, ensuring a solid foundation for design optimization and accurate sizing of the catalytic PFHX.

Additionally, the design procedure for centrifugal compressors and radial turbo-expanders can be further improved by incorporating stage loss calculations into the design flowchart. This will enhances accuracy in estimating isentropic efficiencies and provides additional geometric parameters for further technical assessment and detailed equipment designs. It is important to emphasize that even though the centrifugal compressors designed in this study have successfully met the preliminary design constraints derived from existing industrial limitations, this type of compressors are not yet utilized in industrial hydrogen liquefiers [20,24]. Other critical aspects of centrifugal compressors design, including sealing and lubrication systems, must also be carefully considered to ensure full confidence in the technical feasibility of this equipment for large-scale pure-hydrogen compression.

The same considerations apply to radial turbines, where bearing technology selection is crucial. Most modern hydrogen liquefiers use static or dynamic gas bearings, which eliminate oil contamination risks, reduce space requirements, and offer higher reliability [4,20,44]. The availability of this technology for the large-scale cryogenic plant described in this study needs to be verified.

The economic assessment and projection conducted as part of this research underscore the viability and economic potential of large-scale hydrogen liquefaction. A notable contribution is the development of an updated cost scaling curve, featuring cost estimations for hydrogen liquefiers with capacities of up to 500 TPD—a novel addition to existing literature.

For practical application, the authors encourage the adoption of the proposed framework for assessing the viability of other promising large-scale hydrogen liquefaction processes, such as the reverse-Brayton cycle. Additionally, the authors emphasize the need for continuous refinement in cost estimation models as more accurate data becomes available, given the lack of actual project data used in this study. This ongoing refinement will ensures accurate economic assessment and enhance forecasting ability for the growing hydrogen economy.

In conclusion, the technical and techno-economic assessment in this research suggest that large-scale HP-H_2 Claude cycle hydrogen liquefaction concept has the potential to meet the liquefaction cost target of US\$1/kg_{LH_2}, making it a cost-effective solution for hydrogen transportation and storage. However, there is room for improvement in the developed framework, particularly in enhancing equipment design methodologies, refining cost estimations, and implementing optimization techniques. These advancements will contribute to making hydrogen a more accessible and viable energy carrier for the future.

Software and processing codes

The processing algorithm used in the equipment preliminary designs can be found in the following GitHub repository: https://github.com/pbtamarona/h2liquefaction.

Design results

The results of the preliminary designs of the main process equipment can be found in the following GitHub repository: https://github.com/pbtamarona/h2liquefaction.

CRediT authorship contribution statement

Panji B. Tamarona: Writing – original draft, Visualization, Software, Methodology, Investigation, Formal analysis. **Rene Pecnik:** Writing – review & editing, Supervision, Methodology. **Mahinder Ramdin:** Writing – review & editing, Supervision, Methodology, Conceptualization.

Declaration of competing interest

The authors declare that they have no known competing financial interests or personal relationships that could have appeared to influence the work reported in this paper.

Nomenclature

Abbreviations

H_2	Hydrogen
LH_2	Liquid hydrogen
LN_2	Liquid nitrogen
APEA	Aspen Process Economic Analyzer
CAPEX	Capital expenditure
CEPCI	Chemical Engineering Plant Cost Index
EDR	Exchanger Design and Rating
EOS	Equation of state
EU	European Union
HP-H_2	High-pressure hydrogen
HPC	High-pressure compressor
JT	Joule-Thomson
LPC	Low-pressure compressor
MR	Mixed-refrigerant
OPEX	Operating expenditure
PFD	Process flow diagram
PFHX	Plate-fin heat exchanger
SEC	Specific energy consumption
SLC	Specific liquefaction cost
TEA	Techno-economic analysis
TPD	Tonnes per day
TSA	Temperature-swing adsorbers

Symbols

Δh	Change in enthalpy
$\dot{m}$	Mass flowrate
$\dot{V}$	Volumetric flowrate
$\dot{W}$	Work per unit time
v_s	Isentropic velocity ratio
ω_s	Specific speed
ψ_{is}	Isentropic work coefficient
a	Experience curve constant
b	Learning coefficient
C	Capital cost
c	Specific cost; absolute velocity
c_{is}	Spouting velocity
h	Enthalpy
I_{fix}	Fixed annual interest rate
m	Cost curve constant
n	Rotation per minute; cost exponent
P	Pressure
PR	Pressure ratio
q	Cumulative capacity
S	Plant capacity
t_p	Payment period
u	Impeller wheel tip velocity
z	Number of stages

Sub- and Superscripts

0	Initial
1	Rotor inlet; equipment 1
2	Rotor outlet; equipment 2
a	Annual
comp	Compressor
dis	Discharge
in	Inlet
is	Isentropic
out	Outlet
stage	Radial stage
suc	Suction
tot	Total

Appendix A. Supplementary information

Supplementary material related to this article can be found online at https://doi.org/10.1016/j.ijhydene.2024.06.021.

References

[1] International Energy Agency. The future of hydrogen. Tech. rep., International Energy Agency; 2019, URL https://iea.blob.core.windows.net/assets/9e3a3493-b9a6-4b7d-b499-7ca48e357561/The_Future_of_Hydrogen.pdf.

[2] Al Ghafri SZ, Munro S, Cardella U, Funke T, Notardonato W, Trusler JPM, et al. Hydrogen liquefaction: A review of the fundamental physics, engineering practice and future opportunities. Energy Environ Sci 2022;15(7):2690–731. http://dx.doi.org/10.1039/D2EE00099G.

[3] Connelly E, Penev M, Elgowainy A, Hunter Peer Reviewed By C, Burgunder A, Martinez A, et al. DOE hydrogen and fuel cells program record 19001: Current status of hydrogen liquefaction costs. Tech. rep., US Department of Energy; 2019, URL https://www.hydrogen.energy.gov/pdfs/19001_hydrogen_liquefaction_costs.pdf.

[4] Ohlig K, Decker L. The latest developments and outlook for hydrogen liquefaction technology. In: AIP conference proceedings, vol. 1573, 2014, p. 1311–7. http://dx.doi.org/10.1063/1.4860858.

[5] Monterey Gardiner. DOE hydrogen and fuel cells program record 9013: Energy requirements for hydrogen gas compression and liquefaction as related to vehicle storage needs. Tech. rep., US Department of Energy; 2009, URL https://www.hydrogen.energy.gov/pdfs/9013_energy_requirements_for_hydrogen_gas_compression.pdf.

[6] Berstad D, Skaugen G, Wilhelmsen Ø. Dissecting the exergy balance of a hydrogen liquefier: Analysis of a scaled-up claude hydrogen liquefier with mixed refrigerant pre-cooling. Int J Hydrog Energy 2021;46(11):8014–29. http://dx.doi.org/10.1016/j.ijhydene.2020.09.188.

[7] Heuser P-M, Ryberg DS, Grube T, Robinius M, Stolten D. Techno-economic analysis of a potential energy trading link between Patagonia and Japan based on CO2 free hydrogen. Int J Hydrog Energy 2019;44(25):12733–47. http://dx.doi.org/10.1016/j.ijhydene.2018.12.156.

[8] Wijayanta AT, Oda T, Purnomo CW, Kashiwagi T, Aziz M. Liquid hydrogen, methylcyclohexane, and ammonia as potential hydrogen storage: Comparison review. Int J Hydrog Energy 2019;44(29):15026–44. http://dx.doi.org/10.1016/J.IJHYDENE.2019.04.112.

[9] Teichmann D, Arlt W, Wasserscheid P. Liquid organic hydrogen carriers as an efficient vector for the transport and storage of renewable energy. Int J Hydrog Energy 2012;37(23):18118–32. http://dx.doi.org/10.1016/J.IJHYDENE.2012.08.066.

[10] Ishimoto Y, Voldsund M, Nekså P, Roussanaly S, Berstad D, Gardarsdottir SO. Large-scale production and transport of hydrogen from Norway to Europe and Japan: Value chain analysis and comparison of liquid hydrogen and ammonia as energy carriers. Int J Hydrog Energy 2020;45(58):32865–83. http://dx.doi.org/10.1016/J.IJHYDENE.2020.09.017.

[11] Bruce S, Temminghoff M, Hayward J, Schmidt E, Munnings C, Palfreyman D, et al. National hydrogen roadmap: Pathways to an economically sustainable hydrogen industry in Australia. Tech. rep., Australia: CSIRO; 2018, URL https://www.csiro.au/en/work-with-us/services/consultancy-strategic-advice-services/csiro-futures/energy-and-resources/national-hydrogen-roadmap#:~:text=The%20National%20Hydrogen%20Roadmap%20provides,economically%20sustainable%20industry%20in%20Australia.

[12] Watanabe T, Murata K, Kamiya S, Ota K-i. Cost estimation of transported hydrogen, produced by overseas wind power generations. In: Stolten D, Grube T, editors. 18th world hydrogen energy conference 2010. 2010, p. 547–57.

[13] Raab M, Maier S, Dietrich R-U. Comparative techno-economic assessment of a large-scale hydrogen transport via liquid transport media. Int J Hydrog Energy 2021;46(21):11956–68. http://dx.doi.org/10.1016/j.ijhydene.2020.12.213.

[14] Reuß M, Grube T, Robinius M, Preuster P, Wasserscheid P, Stolten D. Seasonal storage and alternative carriers: A flexible hydrogen supply chain model. Appl Energy 2017;200:290–302. http://dx.doi.org/10.1016/J.APENERGY.2017.05.050.

[15] Stolzenburg K, Mubbala R. Hydrogen liquefaction report. Tech. rep., IDEALHY; 2013.

[16] Kamiya S, Nishimura M, Harada E. Study on introduction of CO2 free energy to Japan with liquid hydrogen. Physics Procedia 2015;67:11–9. http://dx.doi.org/10.1016/J.PHPRO.2015.06.004.

[17] Aasadnia M, Mehrpooya M. Large-scale liquid hydrogen production methods and approaches: A review. Appl Energy 2018;212:57–83. http://dx.doi.org/10.1016/J.APENERGY.2017.12.033.

[18] Alekseev A. Hydrogen liquefaction. In: Hydrogen science and engineering : Materials, processes, systems and technology. Weinheim, Germany: Wiley-VCH Verlag GmbH & Co. KGaA; 2016, p. 733–62. http://dx.doi.org/10.1002/9783527674268.ch30.

[19] Cardella U, Decker L, Sundberg J, Klein H. Process optimization for large-scale hydrogen liquefaction. Int J Hydrog Energy 2017;42(17):12339–54. http://dx.doi.org/10.1016/j.ijhydene.2017.03.167.

[20] Cardella UF. Large-scale hydrogen liquefaction under the aspect of economic viability. 2018, URL https://mediatum.ub.tum.de/604993?query=hydrogen+liquefaction&show_id=1442078&sortfield1=&srcnodeid=604993&sortfield0=author.fullname_comma. https://mediatum.ub.tum.de/doc/1442078/1442078.pdf.

[21] Van Hoecke L, Laffineur L, Campe R, Perreault P, Verbruggen SW, Lenaerts S. Challenges in the use of hydrogen for maritime applications. Energy Environ Sci 2021;14(2):815–43. http://dx.doi.org/10.1039/D0EE01545H.

[22] Krasae-In S. Optimal operation of a large-scale liquid hydrogen plant utilizing mixed fluid refrigeration system. Int J Hydrog Energy 2014;39(13):7015–29. http://dx.doi.org/10.1016/j.ijhydene.2014.02.046.

[23] Skaugen G, Berstad D, Wilhelmsen Ø. Comparing exergy losses and evaluating the potential of catalyst-filled plate-fin and spiral-wound heat exchangers in a large-scale claude hydrogen liquefaction process. Int J Hydrog Energy 2020;45(11):6663–79. http://dx.doi.org/10.1016/j.ijhydene.2019.12.076.

[24] Ohlig K, Decker L. Hydrogen, 4. Liquefaction. In: Ullmann's encyclopedia of industrial chemistry. Weinheim, Germany: Wiley-VCH Verlag GmbH & Co. KGaA; 2013, p. 1–6. http://dx.doi.org/10.1002/14356007.o13_o05.pub2.

[25] Lemmon EW, Bell IH, Huber ML, McLinden MO. NIST standard reference database 23: Reference fluid thermodynamic and transport properties-REFPROp, version 10.0. National Institute of Standards and Technology; 2018, http://dx.doi.org/10.18434/T4/1502528, URL https://www.nist.gov/srd/refprop.

[26] Leachman JW, Jacobsen RT, Penoncello SG, Lemmon EW. Fundamental equations of state for parahydrogen, normal hydrogen, and orthohydrogen. J Phys Chem Ref Data 2009;38(3):721–48. http://dx.doi.org/10.1063/1.3160306.

[27] Valenti G, Macchi E, Brioschi S. The influence of the thermodynamic model of equilibrium-hydrogen on the simulation of its liquefaction. Int J Hydrog Energy 2012;37(14):10779–88. http://dx.doi.org/10.1016/j.ijhydene.2012.04.050.

[28] Lasala S, Privat R, Arpentinier P, Jaubert J-N. Note on the inconsistent definition assigned in the literature to the heat capacity of the so-called equilibrium hydrogen mixture. Fluid Phase Equilib 2020;504:112325. http://dx.doi.org/10.1016/j.fluid.2019.112325.

[29] Häring H-W. Industrial gases processing. Wiley; 2007, http://dx.doi.org/10.1002/9783527621248.

[30] ALPEMA. The standards of the brazed aluminium plate-fin heat exchanger manufacturers' association. 2012.

[31] O'Neill KT, Al Ghafri S, da Silva Falcão B, Tang L, Kozielski K, Johns ML. Hydrogen ortho-para conversion: Process sensitivities and optimisation. Chem Eng Process - Process Intensif 2023;184. http://dx.doi.org/10.1016/j.cep.2023.109272.

[32] Towler G, Sinnott R. Transport and storage of fluids. Chem Eng Des 2013;1207–65. http://dx.doi.org/10.1016/B978-0-08-096659-5.00020-1.

[33] Bloch HP, Soares C. Turboexpanders and process applications. Elsevier; 2001, http://dx.doi.org/10.1016/B978-0-88415-509-6.X5000-4.

[34] Timmerhaus KD, Flynn TM. Equipment associated with low-temperature systems. In: Cryogenic process engineering. Boston, MA: Springer US; 1989, p. 189–285. http://dx.doi.org/10.1007/978-1-4684-8756-5_5.

[35] Gambini M, Vellini M. Turbomachinery selection. In: Turbomachinery: fundamentals, selection and preliminary design. Springer Cham; 2021, p. 89–107. http://dx.doi.org/10.1007/978-3-030-51299-6_2.

[36] Gambini M, Vellini M. Preliminary design of centrifugal compressors. In: Turbomachinery: Fundamentals, selection and preliminary design. Springer Cham; 2021, p. 255–308. http://dx.doi.org/10.1007/978-3-030-51299-6_6.

[37] Gambini M, Vellini M. Preliminary design of radial inflow turbines. In: Turbomachinery: Fundamentals, selection and preliminary design. Springer Cham; 2021, p. 199–253. http://dx.doi.org/10.1007/978-3-030-51299-6_5.

[38] van Lier L, Tumer C, Tedesco M, Buijs L. Hydrogen compression boosting the hydrogen economy. Tech. rep., 2022, European Forum for Reciprocating Compressors.

[39] Brun K, Simons S. Compression options for the hydrogen economy. Gas Compression Mag 2021.

[40] Bahadori A. Gas compressors. In: Natural gas processing. Elsevier; 2014, p. 223–73. http://dx.doi.org/10.1016/B978-0-08-099971-5.00005-2.
[41] Dixon SL, Hall CA. Fluid mechanics and thermodynamics of turbomachinery. 7th ed.. Elsevier; 2014, http://dx.doi.org/10.1016/C2011-0-05059-7.
[42] Elliott H, Bloch H. Compressor technology advances. De Gruyter; 2021, http://dx.doi.org/10.1515/9783110678765.
[43] Bischoff S, Decker L. First operating results of a dynamic gas bearing turbine in an industrial hydrogen liquefier. In: AIP conference proceedings, vol. 1218, 2010, p. 887–94. http://dx.doi.org/10.1063/1.3422445.
[44] Ohlig K, Bischoff S. Dynamic gas bearing turbine technology in hydrogen plants. In: AIP conference proceedings, vol. 1434, 2012, p. 814–9. http://dx.doi.org/10.1063/1.4706994.
[45] Campbell JM, Lilly LL, Maddox RN. Gas conditioning and processing : Volume 2 : The equipment modules. 8th ed.. Norman, Okla: Campbell, cop.; 2000.
[46] Essler J, Haberstroh C, Walnum HT, Berstad D, Nekså P, Stang J, et al. Report on technology overview and barriers to energy- and cost-efficient large scale hydrogen liquefaction. Tech. rep. Idealhy, 2012.
[47] Aspen Technology. Aspen icarus V12 reference guide - APEA. 2021, URL https://esupport.aspentech.com/S_Article?id=000098074.
[48] Towler G, Sinnott R. Capital cost estimating. Chem Eng Des 2013;307–54. http://dx.doi.org/10.1016/B978-0-08-096659-5.00007-9, URL https://linkinghub.elsevier.com/retrieve/pii/B9780080966595000079.
[49] Towler G, Sinnott R. Capital cost estimating. In: Chemical engineering design. Elsevier; 2022, p. 239–78. http://dx.doi.org/10.1016/B978-0-12-821179-3.00007-8.
[50] Syed MT, Sherif SA, Veziroğlu TN, Sheffield JW. An economic analysis of three hydrogen liquefaction systems. Int J Hydrog Energy 1998;23(7):565–76. http://dx.doi.org/10.1016/S0360-3199(97)00101-8.
[51] Fares R. Wind energy is one of the cheapest sources of electricity, and it's getting cheaper. 2017, URL https://blogs.scientificamerican.com/plugged-in/wind-energy-is-one-of-the-cheapest-sources-of-electricity-and-its-getting-cheaper/.
[52] Servet Yanatma. Energy crisis in europe: Which countries have the cheapest and most expensive electricity and gas? 2023, URL https://www.euronews.com/next/2023/03/29/energy-crisis-in-europe-which-countries-have-the-cheapest-and-most-expensive-electricity-a.
[53] Berstad DO, Stang JH, Nekså P. Comparison criteria for large-scale hydrogen liquefaction processes. Int J Hydrog Energy 2009;34(3):1560–8. http://dx.doi.org/10.1016/j.ijhydene.2008.11.058.
[54] Tahan MR. Recent advances in hydrogen compressors for use in large-scale renewable energy integration. 2022, http://dx.doi.org/10.1016/j.ijhydene.2022.08.128.
[55] Khan MA, Young C, Mackinnon CB, Layzell DB. The techno-economics of hydrogen compression. 2021, URL www.transitionaccelerator.ca.
[56] Di Bella Francis A. Development of a centrifugal hydrogen pipeline gas compressor. 2015.
[57] Heshmat H, Sutherland E, Randolph K. Oil-free centrifugal hydrogen compression technology demonstration - DOE hydrogen and fuel cells program FY 2014 annual progress report. Tech. rep., US DOE, Albany, NY: Mohawk Innovative Tachnology Inc.; 2014.
[58] Heshmat H. Oil-free centrifugal hydrogen compression technology demonstration final report prepared for department of energy hydrogen and fuel cells program principal investigator. Tech. rep., Albany, NY: Mohawk Innovative Technology, Inc; 2014, URL www.miti.cc.
[59] Amos WA. Costs of storing and transporting hydrogen. Tech. rep., Golden, CO (United States): National Renewable Energy Laboratory (NREL); 1999, http://dx.doi.org/10.2172/6574.
[60] Yang C, Ogden J. Determining the lowest-cost hydrogen delivery mode. Int J Hydrog Energy 2007;32(2):268–86. http://dx.doi.org/10.1016/j.ijhydene.2006.05.009.
[61] Chen T-P. Nexant, Air Liquide, Chevron Technology Venture, Gas Technology Institute, NREL, Tiax, ANL, hydrogen delivery infrastructure options analysis. Tech. rep., US Department of Energy, URL https://www.osti.gov/servlets/purl/982359.
[62] Elgowainy A, Mintz M, Gillette J, Ringer MN, Brown DP. Hydrogen delivery scenario analysis model (HDSAM) V2.0. 2006, URL https://www.hydrogen.energy.gov/docs/12022c_hdsam2-31_2020_case.xls.
[63] Elgowainy A, Reddi K, Brown DP, Rustagi NDFCTO, Mintz MA, Gillette JA, et al. Hydrogen delivery scenario analysis model (HDSAM) V4.0. 2022, URL https://hdsam.es.anl.gov/.
[64] EERE. Multiyear research, development and demonstration plan - Section 3.2 hydrogen delivery. Tech. rep., EERE Publication and Product Library; 2012, http://dx.doi.org/10.2172/1219578.
[65] Nemet GF. Beyond the learning curve: factors influencing cost reductions in photovoltaics. Energy Policy 2006;34(17):3218–32. http://dx.doi.org/10.1016/J.ENPOL.2005.06.020.
[66] Samadi S. The experience curve theory and its application in the field of electricity generation technologies – A literature review. Renew Sustain Energy Rev 2018;82:2346–64. http://dx.doi.org/10.1016/J.RSER.2017.08.077.
[67] Roser M. Learning curves: What does it mean for a technology to follow Wright's law? 2023, URL https://ourworldindata.org/learning-curve.